



CuPt and CuPtRu Nanostructures for Ammonia Oxidation Reaction

R. H. Manso, J. X. Wang

To be published in "ECS Transactions"

April 2018

Chemistry Department

Brookhaven National Laboratory

U.S. Department of Energy

USDOE Office of Science (SC), Basic Energy Sciences (BES) (SC-22)

Notice: This manuscript has been authored by employees of Brookhaven Science Associates, LLC under Contract No. DE-SC0012704 with the U.S. Department of Energy. The publisher by accepting the manuscript for publication acknowledges that the United States Government retains a non-exclusive, paid-up, irrevocable, world-wide license to publish or reproduce the published form of this manuscript, or allow others to do so, for United States Government purposes.

DISCLAIMER

This report was prepared as an account of work sponsored by an agency of the United States Government. Neither the United States Government nor any agency thereof, nor any of their employees, nor any of their contractors, subcontractors, or their employees, makes any warranty, express or implied, or assumes any legal liability or responsibility for the accuracy, completeness, or any third party's use or the results of such use of any information, apparatus, product, or process disclosed, or represents that its use would not infringe privately owned rights. Reference herein to any specific commercial product, process, or service by trade name, trademark, manufacturer, or otherwise, does not necessarily constitute or imply its endorsement, recommendation, or favoring by the United States Government or any agency thereof or its contractors or subcontractors. The views and opinions of authors expressed herein do not necessarily state or reflect those of the United States Government or any agency thereof.

CuPt and CuPtRu Nanostructures for Ammonia Oxidation Reaction

R. H. Manso^a, L. Song^b, Z. Liang^b, J. X. Wang^b, and J. Chen^a

Liquid fuels, such as methanol, ethanol, and ammonia, are attractive alternative to hydrogen for fuel cells due to their lower costs for storage and distribution. Lack of sufficiently active catalysts for their oxidation reactions is a roadblock. Our previous study found that Pt₃Cu nanodendrites yielded higher activity and durability than Pt nanoparticles for methanol oxidation reaction (MOR) in acid. In this study, we synthesized two types of nanostructures of CuPt and CuPtRu catalysts via seed-mediated growth of Pt and Ru on Cu and tested their performance for ammonia oxidation reaction (AOR) in alkaline solution. Unlike for MOR, the nanodendrites do not promote AOR activity - CuPt performs similar to Pt and CuPtRu is less active than Pt. Interestingly, the AOR peak current is increased by 64% on CuPt nanowires and 330% on CuPtRu nanowires as compared to Pt nanoparticles. These results suggest that AOR prefers extended surface on long nanowires, distinctly differing from MOR. This can be contributed to two factors: NH₃ oxidization to N₂ involves dimerization of two N-containing intermediates to form the N-N bond and diffusion batters for adsorbed intermediates are generally lower on terrace than at low-coordination sites. This demonstrated strong effect of surface morphology will be further studied and utilized in developing advanced AOR nanocatalysts.

Introduction

Previous studies have shown that Pt is active for AOR in alkaline media, $2NH_3 + 6OH^- = N_2 + 6H_2O + 6e^-$, in a narrow potential window. ¹⁻³ The onset potential above 0.4 V versus RHE is due to the activation barrier for deprotonation of NH_3 to NH_2^* , and the AOR current peaks about 0.65 V is because fully deprotonated N^* intermediate formed at high potentials is inactive for dimerization and blocks surface sites. ⁴ Cu is inactive over the entire potential region because its binding to N species is too weak and thus the potential for deprotonation is too high. Ru is at the other extreme. Strong adsorption of N species on Ru facilitates deprotonation, but causes difficult for dimerization of two partially deprotonated intermediates, resulting in a quick deactivation by inactive reaction intermediates. Studies of metal alloys with Pt also found that the AOR peak current on Pt was reduced by alloying with Cu^5 or Ru^1 .

In this study, our goal is to explore the effects of core-shell metal distribution and surface morphology on the AOR activity of Pt. Using Cu seed-mediated growth of Pt

^a Department of Chemistry and Biochemistry, University of Arkansas, Fayetteville, Arkansas 72701, USA

^b Department of Chemistry, Brookhaven National Laboratory, Upton, New York 11973, USA

followed by acid treatment, a lattice contraction of Pt surface layer can be induced by the Cu core with or without its hollowing out. For studying surface morphology effects, nanodendrites represent the surface rich in low coordination sites and nanowires with micrometer length provide extended surface in one dimension, both with high surface area per Pt mass. We further include Ru in the shell on Cu to study whether the presence of Ru at the surface can promote ammonia deprotonation for lowering the AOR onset potential. Our initial results are presented here.

Experimental Methods

Synthesis of CuPt and CuPtRu Nanoendrites and Nanowires

The core-shell type nanostructures were synthesized using our previously-established, seed-mediated methods.⁶⁻⁸ Briefly, Cu seeds were prepared by adding specific amounts of copper acetylacetonate (Cu(acac)₂), copper chloride (CuCl₂), and dodecylamine (DDA) to a 3-neck 25-mL round-bottom flask equipped with a temperature-controlled, heating mantle and a magnetic stirring plate. The flask was connected to a condenser for cooling and a Schlenk line to maintain air-free conditions. For synthesis of nanodendrites, Cu(acac)₂ (52.4 mg, 0.20 mmol), CuCl₂ (13.4 mg, 0.010 mmol), and DDA (5 g) were used; for synthesis of nanowires, Cu(acac)₂ (52.4 mg, 0.20 mmol), CuCl₂ (26.8 mg, 0.020 mmol), and DDA (5 g) were used.

The synthesis of Cu seeds was allowed to proceed at 220 °C for 50 min under the protection of argon prior to the addition of the noble metal precursors. For synthesis of CuPt catalysts, platinum acetylacetonate (Pt(acac)₂, 30 mg, 0.076 mmol) in 1 mL of oleylamine (OLAM) was added to the reaction solution. In synthesis of CuPtRu catalysts, Pt(acac)₂ (30 mg, 0.076 mmol) in 1 mL of OLAM and ruthenium chloride (RuCl₃, 15.8 mg, 0.076 mmol) in 1 mL of OLAM were simultaneously added to the reaction solution. The reaction was allowed to proceed additional 90 min at 220 °C. After the reaction, the product was purified by ethanol to remove excess reactants and resuspended in toluene for further ligand removal procedure.

To remove the DDA and OLAM ligands on the surface of the nanostructures, the resulting product was dried in a 2 dr. vial by evaporating the solvent toluene. Then, 1 mL of polyvinylpyrrolidone (PVP, MW 55,000) aqueous solution (2 mg/mL) was add to the vial, followed by adding 2 mL of water. The nanostructures were resuspended in the PVP aqueous solution. Following this step, 2 mL of glacial acetic acid was added to the vial. The reaction vial was placed in a 60 °C oil bath and the reaction was allowed to proceed for 30 h. The product was purified by water and re-dispersed in water for electrochemical characterization.

Electrochemical Measurements for Ammonium Oxidation

The catalyst samples stored in water were sonicated for 1 min to obtain uniform dispersion. Then certain volumes of the dispersed inks were placed onto glassy carbon electrodes (GCE) and dried in air. The platinum group metal (PGM) loadings, i.e. Pt and Ru, for all four samples were controlled to be 40 μ g cm⁻² on the GCE. We also made electrodes with 40 μ g cm⁻² Pt loading using commercial Pt nanoparticles on carbon support (2.6 nm in diameter, 46 wt% Pt from TKK) as a reference for comparison.

Electrochemical measurements were carried out by using a Voltalab PGZ 402 potentiostat. The catalyst-coated GCE was immersed in solution and faced a Pt-flag

counter electrode. A Hg/HgO electrode in 1 M KOH solution was used as the reference electrode, and the zero potential versus RHE was determined by the open circuit potential on Pt in hydrogen-saturated 1 M KOH solution, which was about -921 mV versus Hg/HgO at ambient temperature. Correction of ohmic loss was made by subtracting the product of measured currents and the high-frequency resistance determined from electrochemical impedance spectra acquired at 450 mV versus RHE. The cyclic voltammetry curves were recorded in argon-purged 1 M KOH solution. The AOR polarization curves were measured in 1 M KOH solution saturated with NH₃ by letting argon gas bubble through 28% NH₃ solution before entering the cell, which also kept the solution oxygen-free. At ambient temperature about 23 °C, the polarization curves obtained were similar to those in 0.1 M NH₃. The main advantage of using an NH₃ bubbler is to ensure constant NH₃ concentration over hours during measurements of different samples because loss of vaporized NH₃ occurs with inert gas flowing through the cell, which is needed for keeping solution free of oxygen.

Results and Discussion

Composition of the CuPt and CuPtRu Nanostructures

The compositions of the CuPt and CuPtRu nanostructures were analyzed by inductively-coupled plasma mass spectrometry (ICP-MS). Table 1 lists the mass concentration (mg/mL) and the atomic percentage (at.%) of each sample. We prepared electrodes with the same PGM loading of 40 µg cm⁻² for each of the four catalysts using the mass concentrations of Pt and Ru listed here. Compared to the Cu:Pt atomic ratios of about 2.7 in the metal precursors, the Cu contents relative to Pt were lowered to about 0.65 in these catalysts. This is in part due to the acid treatment, in which Cu dissolution results in hollow structures. Even though Ru:Pt ratios in the precursors were 1.0, actually deposited Ru in making nanodendrites and nanowires was considerably less as indicated by the atomic percentages of Pt are 5 to 8 fold higher than those for Ru. Compared to Pt, less Ru being reduced during the chemical reactions could be attributed to the lower redox potential of Ru³⁺ to Ru. The high Pt:Ru atomic ratio in the final products is desirable since Ru is expected to act as a deprotonation promoter for AOR on Pt.

TABLE I. Composition of CuPt and CuPtRu nanostructures analyzed by ICP-MS.

Sample	Sample	Cu	Pt	Ru	Cu	Pt	Ru
#	Name	(mg/mL)	(mg/mL)	(mg/mL)	(at.%)	(at.%)	(at.%)
1	CuPtRu ND	0.139	0.745	0.075	32.4	56.6	11.0
2	CuPt ND	0.139	0.660	-	39.3	60.7	-
3	CuPtRu NW	0.122	0.515	0.037	39.0	53.7	7.3
4	CuPt NW	0.180	0.678	-	44.9	55.1	-

ND stands for nanodendrites and NW stands for nanowires.

Morphology of the CuPt and CuPtRu Nanostructures

Figure 1 shows the transmission electron microscopy (TEM) images of nanodendrites of CuPt and CuPtRu and nanowires of CuPt and CuPtRu. The nanodendrites are ~25 nm in size with branches of connected smaller solid or hollow particles. The nanowires were several micrometers long with a diameter of tens nanometers. Both nanowire samples contained some nanoparticles as by-products. Compared to CuPt nanowires, the CuPtRu

nanowires were thicker. These images support that the nanodendrites are rich in low-coordination sites while nanowires provide one-dimension extended surface.

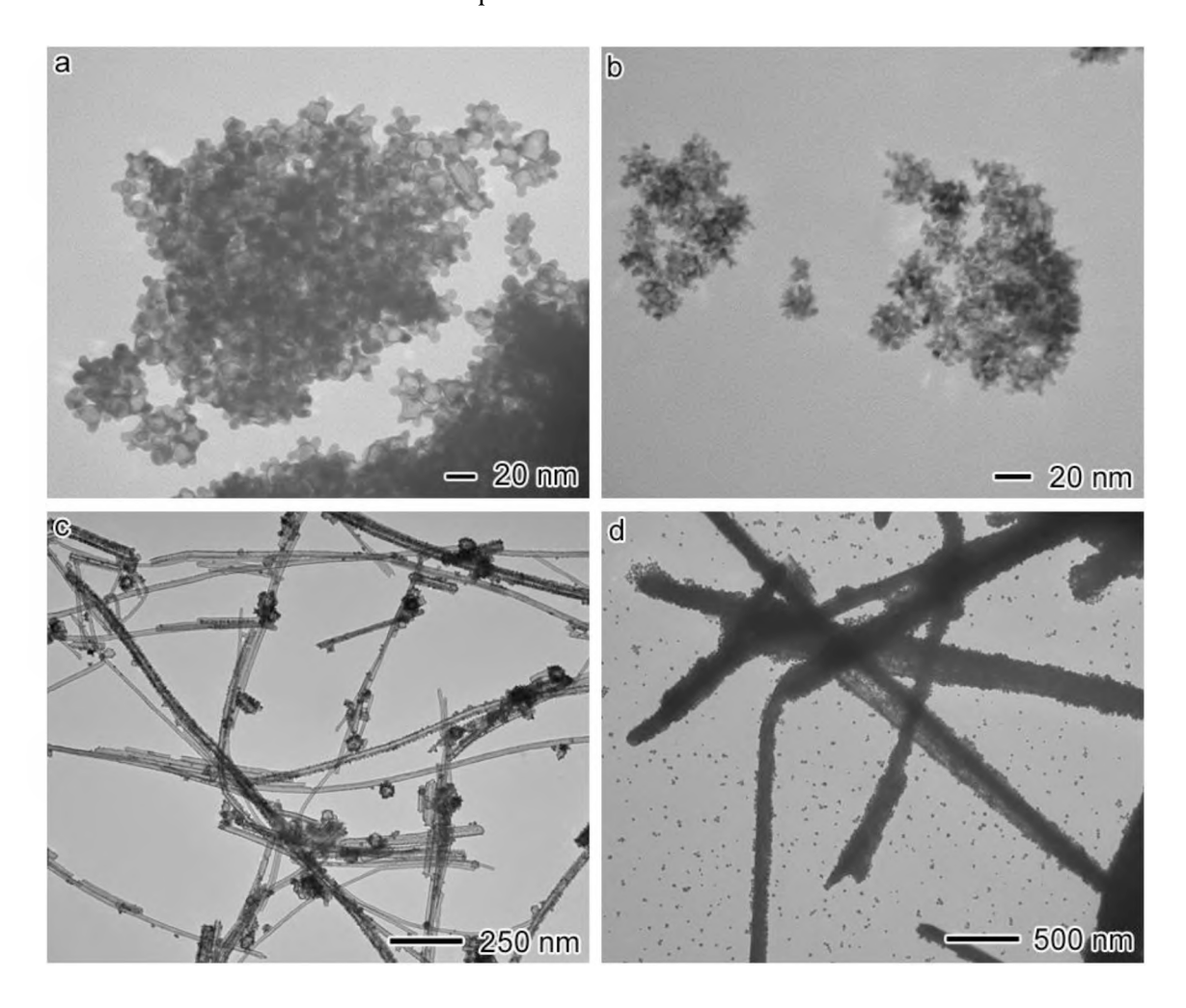


Figure 1. TEM images of CuPt nanodendrites (a), CuPtRu nanodendrites (b), CuPt nanowires (c), and CuPtRu nanowires (d).

Voltammetry and AOR polarization results

In Fig. 2a, we compared the voltammetry curves of CuPt and CuPtRu nanodendrites with that carbon supported Pt nanoparticles. The black curve shows the characteristic voltammetry feature of Pt, i.e., H adsorption/desorption current peaks at low potentials and OH adsorption/desorption current peaks at high potentials. These features are considerably altered on CuPt nanodendrites (blue curve), suggesting that Cu is partly exposed and involved in the surface electrochemical reactions. In contrast, the voltammetry curve for CuPt nanowires (green curve in Fig. 2b) is similar to that of for Pt/C (black curve), indicating there is less exposed Cu. For the CuPtRu samples, large capacitance-like currents were observed for both nanodendrites (pink curve in Fig. 2a) and nanowires (red curve in Fig. 2b), which were consistent with having Ru at the surface. The higher currents for the CuPtRu nanowires (red curve in Fig. 2b) than CuPt nanowires (green curve in Fig. 2b) may result from more attached small particulates on the nanowire surface (Fig. 1c and 1d).

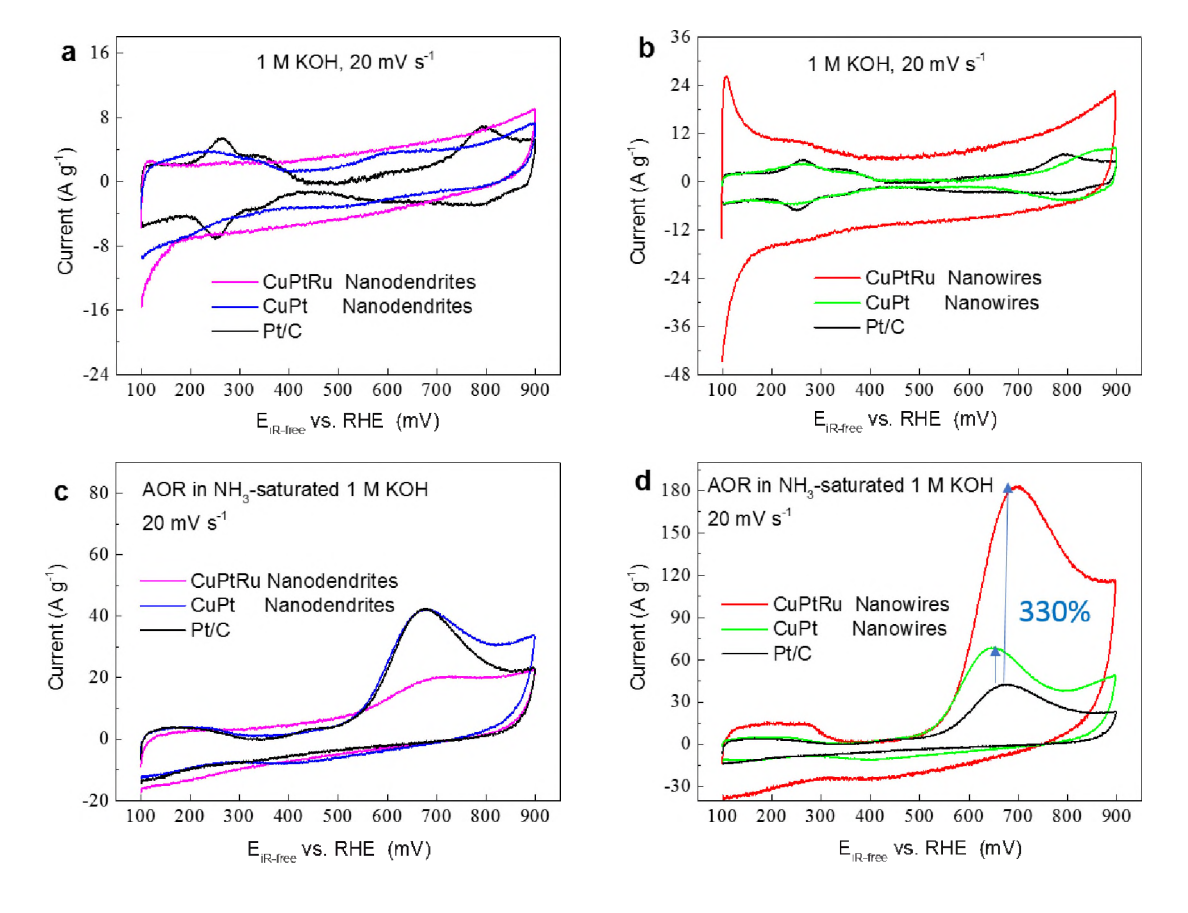


Figure 2. Voltammetry curves measured at ambient temperature about 23 °C in 1 M KOH (a,b) and AOR polarization curves measured in ammonia-saturated 1 M KOH (c,d) for nanostructured catalysts (color lines) compared to Pt nanoparticles on carbon support (black lines). Currents are normalized to the PGM loading.

The AOR polarization measured in NH₃-saturated 1 M KOH solution are shown in Fig. 2c and 2d for the samples of nanodendrites and nanowires, respectively. The CuPt nanodendrites (blue curve in Fig. 2c) exhibit an AOR activity similar to that of Pt/C (black curve), suggesting that lattice contraction of Pt induced by Cu core or hollow structure has little effect on the AOR activity. The CuPtRu nanodendrites are less active than Pt/C for the AOR (pink curve). The negative impact of Ru is similar to that found with Pt-Ru alloy.⁵

Interestingly, situation differs completely for the nanowire samples. As shown in Fig. 2d, the AOR peak current is increased by 330% on CuPtRu nanowires (red curve) and 64% on CuPt nanowires (green curve) compared to that obtained on Pt/C (black curve). Since both nanowire samples enhance the AOR activity and the two nanodendrites performed poorly, extended surface is demonstrated to be more beneficial than low coordination sites for AOR. This is understandable because NH₃ oxidization to N₂ involves dimerization of two N-containing intermediates in the formation of N-N bond and low diffusion barrier on terrace facilities the reactions among adsorbed intermediates. In contrast, oxidation of CH₃OH or C₂H₅OH to CO₂ does not involve combination of two adsorbed intermediates, and thus, nanodendrites have been found promoting the activity for methanol oxidation. It is particularly intriguing that the presence of Ru in nanowires positively impact on the AOR activity. Further studies are required to understand the role of surface Ru, either on the surface of nanowires or on the attached small particulates.

Conclusions

We synthesized CuPt and CuPtRu nanodendrites and nanowires with a seed-mediated method to explore the effects of core-shell metal distribution and surface morphology on the AOR activity of Pt. The most interesting finding is a high AOR peak current of 180 A g⁻¹ on CuPtRu nanowires, which is four times of that on Pt/C. With Cu and Ru both are AOR-inactive metals, the result illustrates that AOR kinetic is sensitive to surface morphology. While it is understandable for extended surface being beneficial for AOR, the role of attached small particulates opens many possibilities. The results warrant us to further explore and rationally design one-dimensional structures for enhancing the AOR performance.

Acknowledgments

The synthesis and structural characterization carried out at University of Arkansas were funded by the National Science Foundation under Grant No. 1703827 and the electrochemical studies performed at Brookhaven National Laboratory were funded by the Advanced Research Projects Agency-Energy (ARPA-E), U.S. Department of Energy, under Award Number DE-AR0000805 and the Division of Chemical Sciences, Geosciences and Biosciences Division, US Department of Energy under contract DE-SC0012704.

References

- 1. F. J. Vidal-Iglesias, J. Solla-Gullón, V. Montiel, J. M. Feliu, and A. Aldaz, *J. Power Sources*, **171**, 448–456 (2007).
- 2. A. C. A. De Vooys, M. T. M. Koper, R. A. Van Santen, and J. A. R. Van Veen, *J. Electroanal. Chem.*, **506**, 127–137 (2001).
- 3. Z.-F. Li, Y. Wang, and G. G. Botte, *Electrochim. Acta*, 228, 351–360 (2017).
- 4. A. Herron et al., J. Phys. Chem. C, 119, 14692–14701 (2015).
- 5. K. Endo, Y. Katayama, and T. Miura, *Electrochim. Acta*, 49, 1635–1638 (2004).
- 6. L. E. Mathurin et al., ChemNanoMat, 4, 76-87 (2018).
- 7. L. E. Mathurin, M. Benamara, J. Tao, Y. Zhu, and J. Chen, Submitted (2018).
- 8. E. Taylor et al., ChemSusChem, 6, 1863–1867 (2013).